and pelleted by centrifugation at 5,000 rpm for 5 min. One of them was treated with α-galactosidase dissolved in sodium citrate/phosphate buffer, and the other tube was treated only with buffer for 1 hr at 37 °C. The cells were washed with the washing solution and treated for 1 hr with FITC/BS-IB_4 on ice. The cells were washed and fixed with 1% paraformaldehyde and analyzed by FCM.

Synonymous (K_S) and non-synonymous (K_A) nucleotide substitutions per site

The number of synonymous substitutions per possible synonymous site (K_S) and the number of non-synonymous substitutions per possible non-synonymous site (K_A) (Li et al., '85; Li, '93) were calculated for codons of full-length α1,3-GT gene and pseudogene sequences using MEGA 2.1 (Kumar et al., 2001). K_A/K_S ratios less than 1.0 are generally considered as evidence that the proteins have evolved under negative or purifying selection; pairwise comparisons between active genes show this pattern (Wolfe and Sharp, '93; Endo et al., '96). K_A/K_S ratios over 1.0 suggest positive or directional selection.

Phylogenetic trees for the α1,3-GT isolates

Two phylogenetic trees using the amino acid sequences and nucleotide sequences of the α1,3-GT cDNAs were constructed using the N–J method (Saitou and Nei, '87), and the reliability of the clusters obtained was evaluated by means of 1,000 bootstrap replicates. The MEGA 2.1 software was used to make the trees.

RESULTS

Isolation of feline α1,3-GT cDNA

A feline kidney cell line, 8C, was used to make α1,3-GT cDNA. Cellular RNA was isolated and reverse transcribed. PCR with the two sets of primers described above was used to amplify cDNA. The PCR product was then ligated with the cloning vector pCR2.1 and the construct was used to transform *E. coli* cells. Plasmid DNAs were isolated from *E. coli* colonies that harbored DNA with the expected length of the insert and used for DNA sequencing. We sequenced seven different clones, and six out of seven clones gave overlapping nucleotide sequences. The full-length coding sequence of the feline α1,3-GT gene was 1,113-bp long (GenBank accession number AY167024) and the deduced amino acid sequence contained 371 amino acids. Its molecular mass was calculated to be 43,568 Da.

Expression of α-galactosyl epitope on the cell surface

The expression vector pcDNA3 with the feline α1,3-GT insert was made and transfected into a cloned human osteosarcoma cell line, HOS, infected with HTLV-I, i.e., HOS/HTLV-I (Hoshino et al., '93) in nine culture wells, and neomycin selection was done. The cells were maintained about 3 weeks in neomycin-containing medium and examined by FCM using fluorescent isothiocyanate-labeled *B. simplicifolia* Isolectin B_4 (FITC/BS-IB_4). In the first screening, FCM results showed that 20–45% cells derived from seven (♯1–♯7) out of nine wells containing the feline α1,3-GT plasmid-transfected cells were positively stained with FITC/BS-IB_4 (Table 1). The cells derived from wells ♯1 and ♯2 were single-cell cloned by seeding them into 96-well plates at a density of one cell per well, and thus obtained two of 19 clones were about 98% positive by FCM (Fig. 1). The clones derived from initial ♯1 and ♯2 wells were designated as HOS/HTLV-I/fGT♯1-a and ♯2-a. The surface expression of α-galactosyl epitopes was stable as it was detected by FCM even after 20 cell passages (data not shown). In contrast, the surface expression of α-galactosyl epitopes was not detected upon FCM of untransfected or only pcDNA3 vector-transfected cells. When the feline α1,3-GT-transduced HOS/HTLV-I cells were treated with α-galactosidase, specific reduction of α-galactosyl epitope expression was detected (Fig. 2) by staining with FITC/BS-IB_4 as compared with results of these cells treated with buffer alone. These findings indicated that the cDNA cloned from 8C cells really coded for the feline α1,3-GT. The cells for highly positive α-galactosyl epitopes grew as well as untransfected HOS/HTLV-I cells, and their morphology was indistinguishable from that of the untransfected HOS/HTLV-I cells.

Analysis of the feline α1,3-GT gene sequence

We aligned the deduced amino acid sequences of the α1,3-GT genes of feline, porcine, murine, bovine, cebus and marmoset origins and the human and orangutan α1,3-GT pseudogenes using software for multiple alignments, Clustal W (Thompson et al., '94) (Fig. 3). In our alignment of the amino acid sequences of the eight α1,3-GT genes, the feline sequence was 85–87% similar to

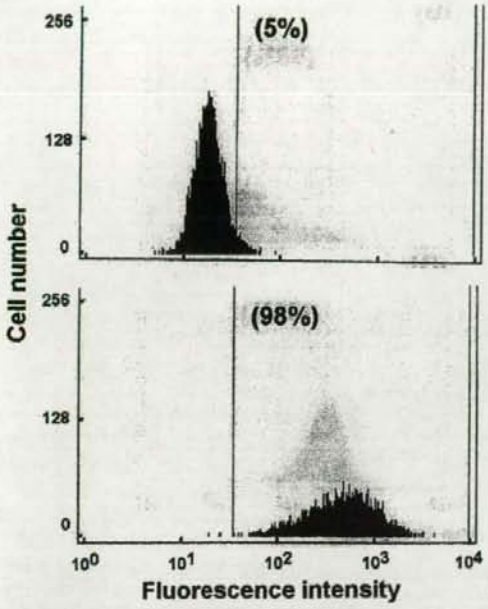

Fig. 1. Detection of α-galactosyl epitope expression. The pcDNA3 control vector-transfected HOS/HTLV-I cells (A) and the feline α1,3-GT gene-transfected HOS/HTLV-I cells (B) were processed for FCM using FITC/BS-IB_4 and examined for the expression of α-galactosyl epitope on the cell surface. The cut-off value for fluorescence intensity was set as 5% of control cells were scored positive (A); the cells that showed stronger intensity than the cut-off value were considered to be positive (B).

those of bovine, porcine, cebus and marmoset origins; the human and orangutan sequences were 82–83% and the murine sequence was 77% similar to the feline sequence. The nucleotide sequences of the bovine, porcine, marmoset and cebus α1, 3-GT genes and of the orangutan and human α1, 3-GT pseudogenes showed a high similarity (88–90%) to the feline sequence, while the murine sequence was only 81% similar to it (Table 2).

Figure 3 shows that there is an especially high similarity among all eight α1,3-GT sequences after amino acid number 84 (feline), 85 (porcine), 85 (murine), 81 (bovine), 89 (human), 89 (cebus), 89 (orangutan) and 90 (marmoset): there was 82–91% similarity in the domain corresponding to amino acid numbers 84–370 of the feline sequence, while in the domain 1–83 the similarity was much lower and between 65% and 72% (Table 2). The highly similar domain has been thought to encode catalytic activities (Henion et al., '94). Although the human and orangutan α1,3-GT genes are inactive, we still noticed the high similarity in their nucleotide sequences with those of other animal α1,3-GT genes. The murine sequence showed a slightly lower similarity: 82% in the 84–370 domain and 62% in the 1–89 domain (Table 2).

To study the evolutionary forces that have been operated among α1,3-GT genes, we analyzed their sequences for synonymous substitution per site (K_S) and non-synonymous substitution per site (K_A) between paired species using the modified Nei–Gojobori method (Kumar et al., 2001). The total number of possible synonymous sites in an individual sequence among the eight α1,3-GT gene sequences was between 287 and 296 (standard error between 6 and 8) with an average of 292, and the total number of possible non-synonymous sites was between 795 and 810 (standard error between 7 and 16) with an average of 803 (data not shown). The total number of possible synonymous and non-synonymous sites in an individual sequence was between 1,082 and 1,104 with an average of 1,095. The total synonymous-site differences between paired samples were between 8 and 121 (standard error between 3 and 9) with a mean of 65 (Table 3), and the non-synonymous-site differences were between 12 and 129 (standard error between 3 and 12) with a mean of 69 (Table 4). We found that the range of the paired samples K_S (calculated using MEGA 2.1 software) was 0.028–0.410 (standard error between 0.009 and 0.028) with a mean of 0.223, and the K_A range was 0.015–0.161 (standard error between 0.006 and 0.015) with a mean of 0.086 (data not shown). The K_S values are significantly higher than the K_A values ($P < 0.0005$, according to Student's t-test). Table 5 shows the K_A/K_S ratios where all the values are within a range of 0.219–0.763, indicating that the α1,3-GT genes are in a direction from negative, purifying selection to neutrality. The ratios between the species that express the active enzyme are around 0.2–0.4 and those of primates, including cebus, orangutan and human but not marmoset, are around 0.7–0.8 irrespective of whether the enzyme is active (cebus) or inactive (orangutan and human). The marmoset α1,3-GT gene shows an intermediate type: 0.273 with that of cebus and about 0.7–0.8 with that of orangutan and human (Table 5).

Phylogenetic trees of the α1,3-GT genes

To analyze the evolutionary distance among α1,3-GT genes of feline, murine, bovine, porcine,

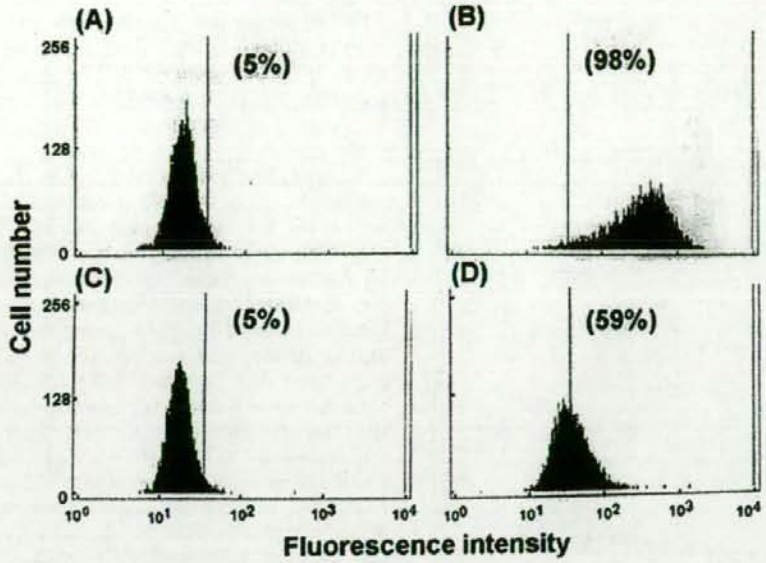

Fig. 2. Detection of α-galactosyl epitope expression. The pcDNA3 vector-transfected HOS/HTLV-I and the feline α1,3-GT plasmid-transfected HOS/HTLV-I cells were initially treated with buffer (**A** and **B**) alone or α-galactosidase (**C** and **D**). The cells were then processed for FCM (as described in Fig. 1) and examined for the expression of α-galactosyl epitope on the cell surface.

cebus and marmoset origins and the α1,3-GT pseudogenes in orangutan and human species, we constructed phylogenetic trees for these α1,3-GT genes and pseudogenes by the N–J method (Saitou and Nei, '87) using the total coding nucleotide sequences (date not shown) and the amino acid sequences (Fig. 4). When the feline α1,3-GT nucleotide sequence was aligned with the other α1,3-GT nucleotide sequences and a phylogenetic tree was made with Poisson correction, it was closely related with the other mammalian α1,3-GT nucleotide sequences. The phylogenetic tree showed that the feline α1,3-GT gene clustered with all other mammalian α1,3-GT genes, especially with the porcine and bovine genes, with a bootstrap support of 93% (date not shown).

The phylogenetic tree constructed using the deduced amino acid sequences shown in Fig. 4 reveals a markedly similar pattern to that constructed using the nucleotide sequences. We also aligned 1–83 and 84–370 amino acid sequences of the feline α1,3-GT with all other α1,3-GT amino acid sequences to make two other phylogenetic trees (data not shown). Both of the phylogenetic trees show almost the same pattern as shown in Fig. 4.

DISCUSSION

When HOS/HTLV-I human cells were transfected with the cDNA encoding the feline α1, 3-GT, they became positive for the expression of α-galactosyl epitopes. In addition, α-galactosidase treatment of HOS/HTLV-I cells transfected with the feline α1,3-GT led to specific reduction of α-galactosyl epitope expression (Fig. 2) as detected by staining with FITC/BS-IB_4. The enzymatic removal of α-galactosyl epitopes was, however, incomplete, probably because the reaction was performed at sub-optimal pH to preserve the cell viability as described by Bracy et al. ('98). Thus, newly cloned human cells showed the stable expression of the feline α1,3-GT (Fig. 1), which catalyzes the addition of α-galactosyl epitopes to existing carbohydrate side chains.

According to the general topology of glycosyltransferases (Paulson and Colley, '89; Joziasse et al., '92), it has been reported that there are three domains in the sequences of glycosyltransferases: a cytoplasmic domain, a transmembrane domain and a luminal domain. Henion et al. ('94) have shown that the 67 amino acids from positions

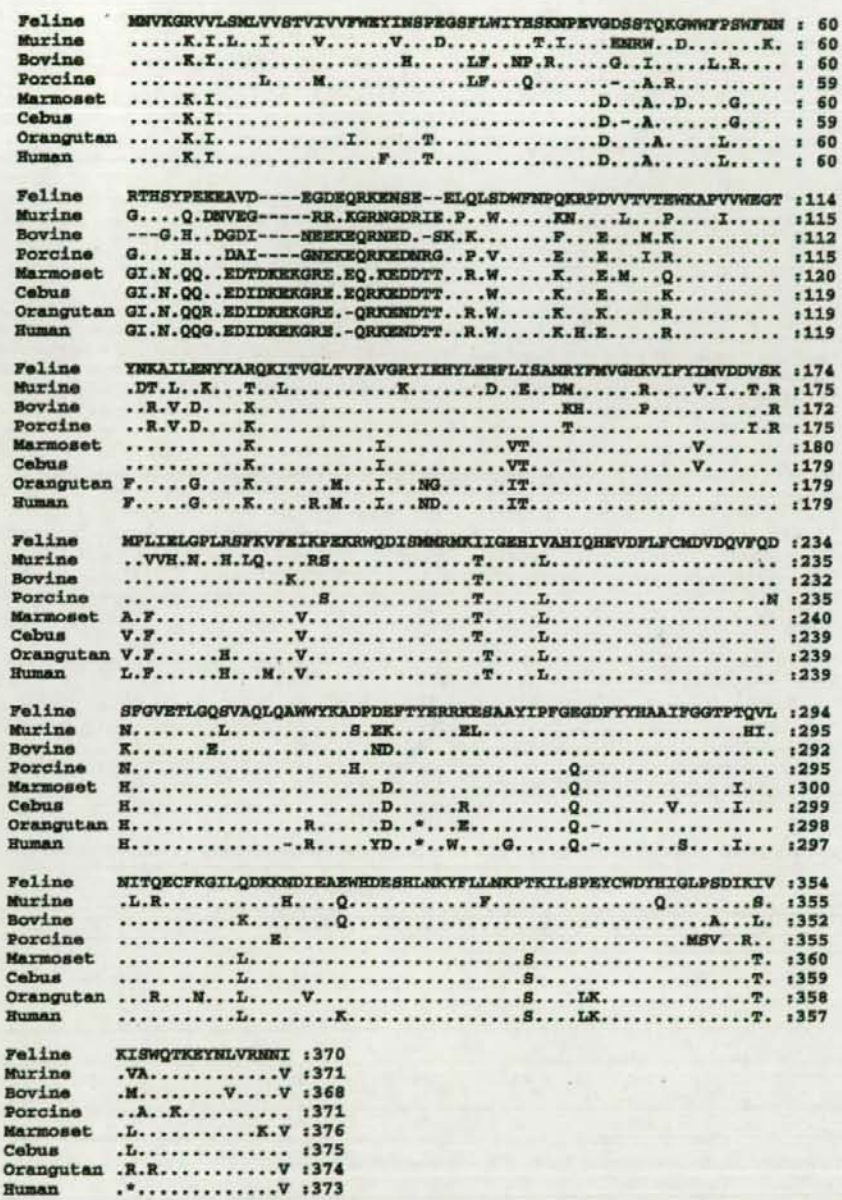

Fig. 3. Alignment of deduced amino acid sequences of different α1,3-GT genes. The amino acid sequences of the feline, porcine, murine, bovine, cebus and marmoset α1,3-GT genes and human and orangutan α1,3-GT pseudogenes are aligned using CLUSTAL W algorithm. Numbers at the right side indicate amino acid positions. Dots (.) represent amino acids identical to those in the feline gene sequence. Amino acid deletions in each gene are indicated by dash marks (-). In the human sequence, the star marks (*) indicate premature stop codons.

TABLE 2. Nucleotide and amino acid similarity between the feline and other α1,3-GT genes

Species	Nucleotide similarity (%)	Amino acid sequence				
		1–83 domain		84–370 domain		Total
		Similarity (%)	Gap	Similarity (%)	Gap	Similarity (%)
Murine	81	62	1[1]	82	0	77
Bovine	88	65	3	90	0	85
Porcine	90	72	1	91	0	87
Marmoset	89	72	0	91	0	87
Cebus	89	72	1	91	0	87
Orangutan	88	70	1	86	1	83
Human	88	70	1	86	2	82

The total coding sequences of the α1,3-GT genes were aligned, including gaps. Identical nucleotides and amino acids at each position, excluding gaps, were counted and a similarity rate (%) was calculated between the feline α1,3-GT gene and each α1,3-GT gene or pseudogene.
[1]Number of amino acid gaps placed when compared with the 1–83 or 84–370 domains of the feline α1,3-GT gene.

TABLE 3. Total number of synonymous differences between paired species among eight different α1,3-GTs

Species	Species							
	Feline	Murine	Bovine	Porcine	Marmoset	Cebus	Orangutan	Human
Feline	—							
Murine	107	—						
Bovine	79	120	—					
Porcine	64	113	61	—				
Marmoset	76	95	74	63	—			
Cebus	71	94	77	61	16	—		
Orangutan	71	87	68	56	17	15	—	
Human	72	91	73	59	21	17	8	—

Total possible synonymous sites were between 287 and 296 with an average of 292.

TABLE 4. Total number of non-synonymous differences between paired species among eight different α1,3-GTs

Species	Species							
	Feline	Murine	Bovine	Porcine	Marmoset	Cebus	Orangutan	Human
Feline	—							
Murine	100	—						
Bovine	62	123	—					
Porcine	51	110	65	—				
Marmoset	48	107	68	64	—			
Cebus	43	106	63	60	12	—		
Orangutan	60	123	83	79	37	34	—	
Human	60	129	83	79	40	36	18	—

Total possible non-synonymous sites were between 795 and 810 with an average of 803.

23 to 89 in the marmoset α1,3-GT gene, which they called a stem region, have little effect on enzymatic activity, but the sequence between 90 and 376 can show an almost full catalytic activity. The presence of stop codons in human and orangutan α1,3-GT genes at the site corresponding to the 268th amino acid of the marmoset gene (Fig. 3) will lead to the loss of about 100 amino acids at the C-terminus. This loss is expected to be sufficient to lose the entire catalytic activity

TABLE 5. K_A/K_S ratios of paired samples among eight different α1,3-GTs

	Species							
Species	Feline	Murine	Bovine	Porcine	Marmoset	Cebus	Orangutan	Human
Feline	—							
Murine	0.343[1]	—						
Bovine	0.284	0.374	—					
Porcine	0.289	0.355	0.386	—				
Marmoset	0.228	0.411	0.335	0.367	—			
Cebus	0.220	0.414	0.298	0.354	0.273	—		
Orangutan	0.306	0.517	0.445	0.510	0.780	0.808	—	
Human	0.304	0.516	0.411	0.485	0.694	0.763	0.786	—

[1] K_A/K_S ratios calculated using MEGA 2.1 software (Kumar et al., 2001).

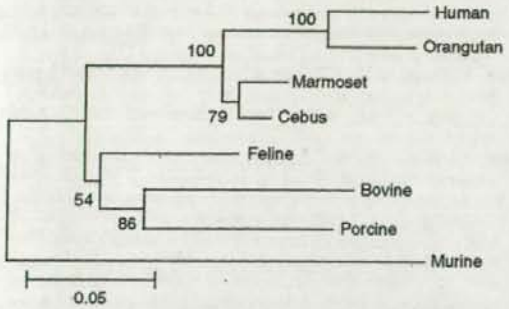

Fig. 4. A phylogenetic tree of the α1,3-GT enzyme. A phylogenetic tree of the amino acid sequences deduced from the nucleotide sequences for murine, feline, porcine, borine, marmoset and cebus α1,3-GT genes and the human and orangutan α1,3-GT pseudogenes was constructed by the N–J method using the MEGA 2.1 software. The phylogenetic relationships of the amino acid sequences are represented as unrooted cladograms. The numbers at branch nodes indicate the bootstrap support level (BSL), which is the percentage of how often each branch presents exactly the same topology in all the resampled trees. The scale bars indicate the number of substitutions per site.

even when α1,3-GT mRNA of human or orangutan is translated.

In our sequence alignment, it appeared that the amino acid residues 61–83 in the feline α1,3-GT gene form a highly variable region and the residues between 84 and 371 form a highly conserved region. This finding also suggests that the catalytic domain of the feline α1,3-GT gene is located in the highly conserved 84–370 domain. In the corresponding domains of animal sequences, including the human and orangutan pseudogenes, the functional constraints appear to have restricted mutations throughout evolution by Wilson et al. ('77). Since most of the amino acid gaps were located between positions 45 and 84 of the feline α1,3-GT sequence, this portion is unlikely to contain catalytic activity.

The α1,3-GT gene is transcribed in a small amount but the enzyme encoded is not active in higher primates (humans, apes and OWM) (Koike et al., 2002): the reason for loss of this enzyme activity in higher primates is unknown. There are several reports on production of α1,3-GT gene-deficient mice (knock-out mice). These mice can grow, live and age normally (Tearle et al., '96; Pearse et al., '98), indicating that the α1,3-GT gene can be dispensable for rodents, although this gene has been evolutionarily conserved as shown in Table 2. On the contrary, the expression of the α1,3-GT gene in human cells did not affect the growth and morphology of human cells, as we could isolate HOS/HTLV-I cell lines highly expressing α1,3-GT (Table 1 and Fig. 1). Thus, its expression did not exert adverse effects on human cells at least in tissue culture. It is intriguing for us that the α1,3-GT genes of marmoset and cebus and the pseudogenes of orangutan and human show similar degrees of substitution rates in their nucleotide sequences as well as in their amino acid sequences to the murine, bovine and porcine genes.

The rate of synonymous substitution (K_S) is usually much higher than that of non-synonymous substitution (K_A) for a normally functioning gene. Synonymous substitution may be used as a molecular clock for dating the evolutionary time of closely related species (Kafatos et al., '77; Kimura, '77; Miyata and Yasunaga, '80; Perler et al., '80). K_A/K_S ratios less than 1.0 are generally taken as negative or purifying selection, and, conversely, K_A/K_S ratios significantly greater than 1.0 are considered to be proper evidence of

directional or positive selection for amino acid replacement (Li et al., '85; Li, '93). That is, when the K_A/K_S value for a given gene is less than 1.0, the encoded protein sequence has been conserved during evolution. For example, the histone H4 gene family protein sequences are under purifying selection (Piontkivska et al., 2002) and some lineages of the primate lysozyme protein sequences are under directional selection (Messier and Stewart, '97). Among the α1,3-GT genes, the synonymous substitution rate is significantly higher than the non-synonymous substitution rate between the paired sequences ($P < 0.0005$). Generally, the values of possible non-synonymous substitutions are much higher than the values of possible synonymous substitutions. Among the α1,3-GT genes we examined, the ranges of possible non-synonymous and synonymous substitution sites were 795–810 and 287–296, respectively.

Pairwise K_A/K_S ratios are high (0.7–0.8) in the species where the enzyme had lost its activity (human or orangutan), but are much lower (0.2–0.4) in the species where the enzyme is active. Although the α1,3-GT gene in marmoset and cebus is active and the K_A/K_S value between them is 0.273, their pairwise K_A/K_S values with human and orangutan pseudogenes are as high as 0.7–0.8. High K_A/K_S values (among human, orangutan and cebus) may indicate that these genes have evolved rapidly at the protein level or tend to evolve free of constraint, although their pairwise K_A/K_S ratios are not greater than 1. It is noteworthy that most of the non-synonymous substitutions are concentrated in a region that locates outside of the catalytic domain of the enzyme (Fig. 3).

Humans are known to carry natural antibodies against α1,3-galactosyl epitope at high titers and these antibodies are also known to markedly affect transplantation of xenografts derived from porcine organs and will lead to rejection (Sandrin and McKenzie, '94). A pig strain with knock-out of this gene has already been made (Dor et al., 2004). These antibodies should, however, be beneficial for survival of higher primates. These natural antibodies have been thought to exert prophylactic effects on development of cancer or infection with certain pathogens bearing α-galactosyl epitope (Gollogly and Castronovo, '96; Welsh et al., '98). It remains to be elucidated why α1,3-GT genes should have been inactivated in humans, apes and OWM and why the inactivated gene sequences still have a high degree of similarity to those of the active genes.

J. Exp. Zool. (Mol. Dev. Evol.) DOI 10.1002/jez.b

ACKNOWLEDGMENTS

We thank Ms. Nakamura for excellent technical assistance. This work was supported in part by Grants-in-Aid for Scientific Research and the 21st Century COE Program from the Ministry of Education, Culture, Sports, Science and Technology of Japan. This work was also supported by Core Research for Evolutional Science and Technology (CREST) from the Japan Science and Technology Corporation.

LITERATURE CITED

Azimzadeh A, Wolf P, Thibaudeau K, Cinqualbre J, Soulillou JP, Anegon I. 1997. Comparative study of target antigens for primate xenoreactive natural antibodies in pig and rat endothelial cells. Transplantation 64:1166–1174.

Basu M, Basu S. 1973. Enzymatic synthesis of a blood group B-related pentaglycosylceramide by an alpha-galactosyltransferase from rabbit bone marrow. J Biol Chem 248:1700–1706.

Blanken WM, Van den Eijnden DH. 1985. Biosynthesis of terminal Gal alpha 1-3Gal beta 1-4GlcNAc-R oligosaccharide sequences on glycoconjugates. Purification and acceptor specificity of a UDP-Gal:N-acetyllactosaminide alpha 1, 3-galactosyltransferase from calf thymus. J Biol Chem 260: 12927–12934.

Bracy JL, Sachs DH, Iacomini J. 1998. Inhibition of xenoreactive natural antibody production by retroviral gene therapy. Science 281:1845–1847.

Dor FJ, Tseng YL, Cheng J, Moran K, Sanderson TM, Lancos CJ, Shimizu A, Yamada K, Awwad M, Sachs DH, Hawley RJ, Schuurman HJ, Cooper DK. 2004. Alpha1,3-galactosyltransferase gene-knockout miniature swine produce natural cytotoxic anti-Gal antibodies. Transplantation 78:15–20.

Elices MJ, Blake DA, Goldstein IJ. 1986. Purification and characterization of a UDP-Gal:beta-D-Gal(1,4)-D-GlcNAc alpha(1,3)-galactosyltransferase from Ehrlich ascites tumor cells. J Biol Chem 261:6064–6072.

Endo T, Ikeo K, Gojobori T. 1996. Large-scale search for genes on which positive selection may operate. Mol Biol Evol 13: 685–690.

Fischinger PJ, Peebles PT, Nomura S, Haapala DK. 1973. Isolation of RD-114-like oncornavirus from a cat cell line. J Virol 11:978–985.

Galili U, Swanson K. 1991. Gene sequences suggest inactivation of alpha-1,3-galactosyltransferase in catarrhines after the divergence of apes from monkeys. Proc Natl Acad Sci USA 88:7401–7404.

Galili U, Rachmilewitz EA, Peleg A, Flechner I. 1984. A unique natural human IgG antibody with anti-alpha-galactosyl specificity. J Exp Med 160:1519–1531.

Galili U, Clark MR, Shohet SB, Buehler J, Macher BA. 1987. Evolutionary relationship between the natural anti-Gal antibody and the Gal alpha 1,3Gal epitope in primates. Proc Natl Acad Sci USA 84:1369–1373.

Galili U, Shohet SB, Kobrin E, Stults CL, Macher BA. 1988. Man, apes, and Old World monkeys differ from other mammals in the expression of alpha-galactosyl epitopes on nucleated cells. J Biol Chem 263:17755–17762.

Gollogly L, Castronovo V. 1996. A possible role for the alpha 1–>3galactosyl epitope and the natural anti-gal antibody in oncogenesis. Neoplasma 43:285–289.

Henion TR, Macher BA, Anaraki F, Galili U. 1994. Defining the minimal size of catalytically active primate alpha 1,3 galactosyltransferase: structure-function studies on the recombinant truncated enzyme. Glycobiology 4:193–201.

Hoshino H, Nakamura T, Tanaka Y, Miyoshi I, Yanagihara R. 1993. Functional conservation of the neutralizing domains on the external envelope glycoprotein of cosmopolitan and melanesian strains of human T cell leukemia/lymphoma virus type I. J Infect Dis 168:1368–1373.

Jinno A, Shimizu N, Soda Y, Haraguchi Y, Kitamura T, Hoshino H. 1998. Identification of the chemokine receptor TER1/CCR8 expressed in brain-derived cells and T cells as a new coreceptor for HIV-1 infection. Biochem Biophys Res Commun 243:497–502.

Joziasse DH. 1992. Mammalian glycosyltransferases: genomic organization and protein structure. Glycobiology 2: 271–277.

Joziasse DH, Shaper JH, Van den Eijnden DH, Van Tunen AJ, Shaper NL. 1989. Bovine alpha 1,3-galactosyltransferase: isolation and characterization of a cDNA clone. Identification of homologous sequences in human genomic DNA. J Biol Chem 264:14290–14297.

Joziasse DH, Shaper JH, Jabs EW, Shaper NL. 1991. Characterization of an alpha 1,3-galactosyltransferase homologue on human chromosome 12 that is organized as a processed pseudogene. J Biol Chem 266:6991–6998.

Joziasse DH, Shaper NL, Kim D, Van den Eijnden DH, Shaper JH. 1992. Murine alpha 1,3-galactosyltransferase. A single gene locus specifies four isoforms of the enzyme by alternative splicing. J Biol Chem 267:5534–5541.

Kafatos FC, Efstratiadis A, Forget BG, Weissman SM. 1977. Molecular evolution of human and rabbit beta-globin mRNAs. Proc Natl Acad Sci USA 74:5618–5622.

Kimura M. 1977. Preponderance of synonymous changes as evidence for the neutral theory of molecular evolution. Nature 267:275–276.

Koike C, Fung JJ, Geller DA, Kannagi R, Libert T, Luppi P, Nakashima I, Profozich J, Rudert W, Sharma SB, Starzl TE, Trucco M. 2002. Molecular basis of evolutionary loss of the alpha 1,3-galactosyltransferase gene in higher primates. J Biol Chem 277:10114–10120.

Kumar S, Tamura K, Jakobsen IB, Nei M. 2001. MEGA2: molecular evolutionary genetics analysis software. Bioinformatics 17:1244–1245.

Larsen RD, Rajan VP, Ruff MM, Kukowska-Latallo J, Cummings RD, Lowe JB. 1989. Isolation of a cDNA encoding a murine UDPgalactose:beta-D-galactosyl-1, 4-*N*-acetyl-D-glucosaminide alpha-1,3-galactosyltransferase: expression cloning by gene transfer. Proc Natl Acad Sci USA 86:8227–8231.

Larsen RD, Rivera-Marrero CA, Ernst LK, Cummings RD, Lowe JB. 1990. Frameshift and nonsense mutations in a human genomic sequence homologous to a murine UDP-Gal:beta-D-Gal(1,4)-D-GlcNAc alpha(1,3)-galactosyltransferase cDNA. J Biol Chem 265:7055–7061.

Li WH. 1993. Unbiased estimation of the rates of synonymous and nonsynonymous substitution. J Mol Evol 36:96–99.

Li WH, Wu CI, Luo CC. 1985. A new method for estimating synonymous and nonsynonymous rates of nucleotide substitution considering the relative likelihood of nucleotide and codon changes. Mol Biol Evol 2:150–174.

Messier W, Stewart CB. 1997. Episodic adaptive evolution of primate lysozymes. Nature 385:151–154.

Miyata T, Yasunaga T. 1980. Molecular evolution of mRNA: a method for estimating evolutionary rates of synonymous and amino acid substitutions from homologous nucleotide sequences and its application. J Mol Evol 16:23–36.

Paulson JC, Colley KJ. 1989. Glycosyltransferases. Structure, localization, and control of cell type-specific glycosylation. J Biol Chem 264:17615–17618.

Pearse MJ, Witort E, Mottram P, Han W, Murray-Segal L, Romanella M, Salvaris E, Shinkel TA, Goodman DJ, d'Apice AJ. 1998. Anti-Gal antibody-mediated allograft rejection in alpha1,3-galactosyltransferase gene knockout mice: a model of delayed xenograft rejection. Transplantation 66:748–754.

Perler F, Efstratiadis A, Lomedico P, Gilbert W, Kolodner R, Dodgson J. 1980. The evolution of genes: the chicken preproinsulin gene. Cell 20:555–566.

Piontkivska H, Rooney AP, Nei M. 2002. Purifying selection and birth-and-death evolution in the histone H4 gene family. Mol Biol Evol 19:689–697.

Saitou N, Nei M. 1987. The neighbor-joining method: a new method for reconstructing phylogenetic trees. Mol Biol Evol 4:406–425.

Sandrin MS, McKenzie IF. 1994. Gal alpha (1,3)Gal, the major xenoantigen(s) recognised in pigs by human natural antibodies. Immunol Rev 141:169–190.

Spiro RG, Bhoyroo VD. 1984. Occurrence of alpha-D-galactosyl residues in the thyroglobulins from several species. Localization in the saccharide chains of the complex carbohydrate units. J Biol Chem 259:9858–9866.

Strahan KM, Gu F, Preece AF, Gustavsson I, Andersson L, Gustafsson K. 1995. cDNA sequence and chromosome localization of pig alpha 1,3-galactosyltransferase. Immunogenetics 41:101–105.

Tearle RG, Tange MJ, Zannettino ZL, Katerelos M, Shinkel TA, Van Denderen BJ, Lonie AJ, Lyons I, Nottle MB, Cox T, Becker C, Peura AM, Wigley PL, Crawford RJ, Robins AJ, Pearse MJ, d'Apice AJ. 1996. The alpha-1,3-galactosyltransferase knockout mouse. Implications for xenotransplantation. Transplantation 61:13–19.

Thall A, Galili U. 1990. Distribution of Gal alpha 1,3Gal beta 1, 4GlcNAc residues on secreted mammalian glycoproteins (thyroglobulin, fibrinogen, and immunoglobulin G) as measured by a sensitive solid-phase radioimmunoassay. Biochemistry 29:3959–3965.

Thompson JD, Higgins DG, Gibson TJ. 1994. CLUSTAL W: improving the sensitivity of progressive multiple sequence alignment through sequence weighting, position-specific gap penalties and weight matrix choice. Nucleic Acids Res 22:4673–4680.

Welsh RM, O'Donnell CL, Reed DJ, Rother RP. 1998. Evaluation of the Galalpha1-3Gal epitope as a host modification factor eliciting natural humoral immunity to enveloped viruses. J Virol 72:4650–4656.

Wilson AC, Carlson SS, White TJ. 1977. Biochemical evolution. Annu Rev Biochem 46:573–639.

Wolfe KH, Sharp PM. 1993. Mammalian gene evolution: nucleotide sequence divergence between mouse and rat. J Mol Evol 37:441–456.

Wood C, Kabat EA, Murphy LA, Goldstein IJ. 1979. Immunochemical studies of the combining sites of the two isolectins, A4 and B4, isolated from *Bandeiraea simplicifolia*. Arch Biochem Biophys 198:1–11.

Available online at www.sciencedirect.com
SCIENCE DIRECT
Microbes and Infection 8 (2006) 105–113
Microbes and Infection
www.elsevier.com/locate/micinf

Original article

Construction and in vitro characterization of a chimeric simian and human immunodeficiency virus with the RANTES gene

Yuya Shimizu [a], Masashi Okoba [a], Nanase Yamazaki [a], Yoshitaka Goto [a], Tomoyuki Miura [b], Masanori Hayami [b], Hiroo Hoshino [c], Takeshi Haga [a,*]

[a] Department of Veterinary Microbiology, University of Miyazaki, 1-1 Kibanadai Nishi, Miyazaki 889-2192, Japan
[b] Laboratory of Primate Model, Experimental Research Center for Infectious Disease, Institute for Virus Research, Kyoto University, 53 Shougoin-kawaharamachi, Sakyo-ku, Kyoto 606-8507, Japan
[c] Department of Virology and Preventive Medicine, Gunma University School of Medicine, 3-39-22 Showa-machi, Maebashi, Gunma 371-8511, Japan

Received 1 February 2005; received in revised form 31 May 2005; accepted 1 June 2005

Available online 09 September 2005

Abstract

Chimeric simian–human immunodeficiency virus (SHIV) containing the *env* gene of HIV-1 infects macaque monkeys and provides basic information that is useful for the development of HIV-1 vaccines. Regulated-on-activation-normal-T-cell-expressed-and-secreted (RANTES), a CC-chemokine, enhances antigen-specific T helper type-1 responses against HIV-1. With the final goal of testing the adjuvant effects of RANTES in SHIV-macaque models, we constructed a SHIV having the RANTES gene (SHIV-RANTES) and characterized its properties in vitro. SHIV-RANTES replicated both in human and monkey T cell lines. Along with SHIV-RANTES replication, RANTES was detected in the supernatant of human and monkey cell cultures, at maximal levels of 98.5 and 4.1 ng/ml, respectively. A flow cytometric analysis showed that the expressed RANTES down-modulated CC-chemokine receptor 5 (CCR5) on PM1 cells, which was restored by adding anti-RANTES antibody. UV-irradiated culture supernatants from the SHIV-RANTES-infected cells suppressed replication of CCR5-tropic HIV-1 BaL in PM-1 cells. Differentiating real-time RT-PCR showed that pre-infection of SHIV-RANTES in C8166 cells expressing CCR5 suppressed the replication of HIV-1 BaL. Biological activity of the expressed RANTES and the inserted RANTES gene in SHIV-RANTES remained stable after 10 passages. These results suggest that SHIV-RANTES is worth testing in macaque models.

Keywords: SHIV; RANTES; HIV-1; AIDS

1. Introduction

A successful HIV-1 vaccine is needed to control the worldwide AIDS epidemic. Chimeric simian and human immunodeficiency virus (SHIV) clones containing the HIV-1 *env* genes on a simian immunodeficiency virus (SIV) provide useful information on HIV-1 vaccine development, because SHIVs are readily infectious to macaque monkeys, and show induction of immune responses to HIV-1 Env. We previously reported the in vivo properties of the SHIV-NM3rN (derived from HIV-1 NL432 and SIV mac239) with deletion in the *vpx*, *vpr*, and/or *nef* genes [1]. Macaque monkeys inoculated with these gene-deleted SHIVs induced anti-HIV-1 Env humoral and cell-mediated immunity without causing an AIDS-like disease [1]. Moreover, the monkeys immunized with the *nef*-deleted SHIVs (SHIV-NI), were protected from a challenge with a heterologous pathogenic SHIV [2,3]. Live-attenuated SIV/SHIVs have been shown to be effective vaccines in macaque models. However, serious questions about the pathogenic potential of live-attenuated SIVs [4,5] have dampened enthusiasm for their use in clinical trials. Nevertheless, clarification of the protective mechanisms of attenuated SIV/SHIVs in macaque models could help to improve other vaccine candidates such as live vector-based vaccines and plasmid-DNA immunogens. In general, the immunogenicity of live-attenuated vaccines tends to increase with increasing virulence [6]. Therefore, in attenuating a live virus, there is a trade-off between safety and immunogenicity. A good way to overcome this problem is to genetically engi-

* Corresponding author. Tel./fax: +81 985 58 7575.
E-mail address: a0d518u@cc.miyazaki-u.ac.jp (T. Haga).

1286-4579/$ - see front matter © 2005 Elsevier SAS. All rights reserved.
doi:10.1016/j.micinf.2005.06.017

neer a virus to co-express an immunostimulatory agent such as a cytokine adjuvant. Several studies have demonstrated that insertion of a cytokine in a gene-deleted live-attenuated SIV could boost its immunogenicity and enhance its protection ability [7,8]. This would make it possible to obtain a higher level of immunogenicity from safer, less virulent strains.

Chemokines constitute a family of small proinflammatory cytokines that regulate the activation and migration of leukocytes. Regulated-on-activation-normal-T-cell-expressed-and-secreted (RANTES) is a CC-chemokine and a natural ligand for the CC-chemokine receptors 1 (CCR1), CCR3, and CCR5. Receptors of RANTES are expressed on a variety of cells predominantly associated with T helper type-1 (Th1) responses [9]. An immune response polarized toward a more Th1 response is associated with a reduced viral load and non-progression of disease in HIV-1 infection. RANTES has been found to enhance cellular immune responses resulting in a more effective immune-modulating effect against HIV-1-related virus in rodent and monkey models [10–13]. In addition, infection of macaques with a live-attenuated SIV induced the production of CC-chemokines [14–16], and the up-regulation of CC-chemokines was found to be associated with the sterilizing immunity generated by the vaccine [14]. Moreover, RANTES has been shown to directly inhibit HIV-1 replication in vitro [17,18]. RANTES blocks or down-modulates CCR5 in vitro, which leads to suppression of CCR5-tropic (R5-tropic) HIV-1 infections. These results make RANTES an attractive candidate as a cytokine adjuvant.

To study the adjuvant effect of RANTES against HIV-1 related-virus infections in the macaque model, we have genetically engineered a SHIV to express the human RANTES gene (SHIV-RANTES). In this study, we compare the in vitro properties of SHIV-RANTES with those of its parental SHIV-NI. SHIV-RANTES replicates in both human and monkey cells, and expresses a high amount of RANTES. The RANTES produced with SHIV-RANTES was biologically active as shown by its ability to down-modulate expression of CCR5 and to inhibit the R5-tropic HIV-1 BaL infection. Pre-inoculating cells with SHIV-RANTES more efficiently suppressed a challenge with R5-tropic HIV-1 BaL in vitro than did pre-inoculation with the parental SHIV-NI. These results suggest that SHIV-RANTES will be useful for understanding the effect of RANTES against HIV-1-related infections. These data are an initial step toward the assessment of SHIV-RANTES in vivo.

2. Materials and methods

2.1. Construction of SHIV-RANTES

The SHIV-*nef* vector, designated as SHIV-NI, was constructed from an infectious molecular clone of SHIV-NM3rN [19]. The *env* gene of the SHIV-NM3rN was derived from CXCR4-tropic (X4-tropic) HIV-1 NL432, whose replication

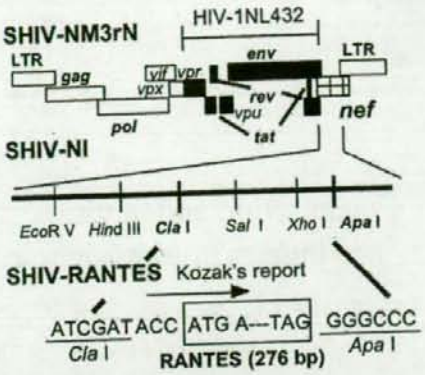

Fig. 1. Genetic structure of SHIV-RANTES. The *Cla* I and *Xho* I region of parental SHIV-NI, the *nef* cassette vector, was replaced by the human RANTES gene. The ORF including the initiation (ATG) and stop (TAG) codons of the RANTES gene is shown in the box. The flanking sequence of the RANTES initiation codon (ACCATGA) is an effective ribosomal initiation sequence based on Kozakn enzyme sites in place of the *nef* gene of SHIV-NM3rN. SHIV-NM3rN was constructed from HIV-1 NL432 's report (effective ribosomal initiation sequence: ANNATGN or GNNATGR). SHIV-NI has some unique restrictio(black regions) and SIV mac239 (white regions).

is not thought to be blocked by RANTES. In SHIV-NI, the *nef* gene was replaced by some unique restriction enzyme sites, including the *Cla* I and *Apa* I sites. The human RANTES open reading frame (ORF) was first amplified by PCR from a full length human RANTES cDNA as previously described [20]. The flanking sequence of the RANTES ORF was modified with the PCR primer RAN-Cla (5'-AT*ATCGAT*-ACCATGAAGGTCTCCGCGGCAG-3') and RAN-Apa (5'-TA*GGGCCC*CTAGCTCATCTCCAAAGAGTTG-3'). The underlined ATG in RAN-Cla indicates the start of the RANTES ORF. The relevant restriction sites in each primer are shown in italics. The flanking sequence of the RANTES initiation codon (ACCATGA) corresponds to an effective ribosomal initiation sequence based on Kozak's [21] report (effective ribosomal initiation sequence, ANNATGN or GNNATGR). The PCR product was cloned into pUC119 vector by TA-cloning, and the sequence was confirmed as previously described [22]. The PCR fragment digested with *Cla* I and *Apa* I was inserted into the SHIV-*nef* vector (Fig. 1).

2.2. Cell cultures

A $CD4^+$ human T lymphoid cell line, M8166 (a subclone of C8166), was used to prepare the stock virus and to measure the viral infectivity in human cells [23]. HSC-F cells, a cynomolgus monkey $CD4^+$ T cell line, were used to assess the viral infectivity in monkey cells [24]. PM1, a $CD4^+$ T cell clone that expresses CCR5, was derived from the human neoplastic T cells line Hut78 [25]. C8166-CCR5 cells were established by the transfection of C8166 cells with the human CCR5 coding region using retrovirus vector pMX-puro, which contains a puromycin-resistant gene [26]. PM1 and C8166-CCR5 were utilized as CCR5-expressing cells and R5-tropic

HIV-1-susceptible cells. These cell lines were all maintained in RPMI medium (RPMI 1640 with 2 mM L-glutamine and sodium bicarbonate; Sigma, St. Louis, MO) containing 10% heat-inactivated fetal calf serum (FCS) (Gibco-BRL Life Technologies, Auckland, New Zealand). Puromycin (1 μg/ml, Sigma) was added to the medium as a selection agent for C8166-CCR5 cells.

2.3. Virus stock

SHIV-RANTES and SHIV-NI was propagated as descried previously [22]. The virus stocks of the SHIV-RANTES and SHIV-NI were produced in M8166 cells, and the virion-associated reverse transcriptase (RT) activity of the virus stocks was measured. The titers of the viruses were determined by the 50% tissue culture infectious dose ($TCID_{50}$) method as described by Reed and Muench [27]. The $TCID_{50}$ of virus was correlated with the RT activity in this study. The laboratory monocytotropic HIV-1 BaL was utilized as R5-tropic HIV-1 [28]. The virus stock of HIV-1 BaL was prepared from the culture supernatants of HIV-1 BaL-infected PM1 cells.

2.4. Virus Infection of human and monkey cells

To investigate the kinetics of virus replication and production of RANTES with SHIV-RANTES in human cells, M8166 cells were inoculated with the virus as described elsewhere [22]. The virus inoculum was adjusted to contain a certain amount of RT units by adding the appropriate volume of the medium to the virus stock. Half of the culture supernatant was harvested with subsequent addition of new medium every 3 days. Virus replication kinetics was monitored by the RT activity of the supernatant. The production of RANTES from the virus-infected cells was measured by enzyme linked immunosorbent assay (ELISA) using a Quantikine human RANTES ELISA kit (R & D Systems, Inc., Minneapolis, MN). To assess the properties of SHIV-RANTES in monkey cells, HSC-F cells were also inoculated with the virus.

2.5. Flow cytometric analysis of CCR5 expression

RANTES down-modulates expression of CCR5 on the cell surface [29]. To assess the biological activity of the RANTES produced by virus-infected M8166 cells, the down-modulation of CCR5 in PM1 cells was evaluated. PM1 cells were plated at 2.5×10^5 cells per well, and incubated for 30 min at 37 °C with 100 μl of the culture supernatant of the samples. Thereafter, the cells were harvested and treated in staining buffer [phosphate buffered saline (PBS) containing 2% FCS and 0.1% sodium azide] for 20 min at 4 °C with phycoerythrin-conjugated anti-human CCR5 monoclonal antibodies (MAb) (2D7: PharMingen, San Diego, CA). To inactivate the virus, the cells were fixed in 4% paraformaldehyde for 30 min. Cells were analyzed for the cell surface expression of CCR5 by flow cytometry (EPICS XL ELITE: Beckman Coulter, Miami, FL). The percentage of CCR5 expression was calculated based on the samples without RANTES (0 ng/ml) which was defined as 100%. To assess the effect of the virus particles, the concentrations of the virions in the culture supernatants from the SHIV-RANTES-infected M8166 cells and SHIV-NI-infected cells were adjusted based on the virion associated-RT activity levels. To evaluate the effect of the spontaneous production of RANTES from the M8166 cells, the CCR5 expression on PM1 cells exposed to supernatants from virus-uninfected cells (hereafter referred to Mock) was also monitored. Serial dilutions of recombinant human RANTES (2–200 ng/ml; CHEMICON International, Inc., Temecula, CA) were used as controls. In the blocking assay with the anti-RANTES neutralizing antibodies, the supernatant samples were incubated with 25 μg/ml of MAb anti-human RANTES (R & D Systems) for 30 min at 37 °C before adding the samples to PM1 cells.

2.6. Inhibition of R5-tropic HIV-1 replication with the RANTES produced by SHIV-RANTES

To investigate whether the produced RANTES inhibits R5-tropic HIV-1 infections, the replication of HIV-1 BaL, an R5-tropic HIV-1, was monitored in the presence of the culture supernatants from the SHIV-RANTES-infected cells. The SHIVs in the culture supernatants were inactivated by UV-irradiation at 2 J/cm^2 to exclude the interference of replication of SHIVs on this assay. PM1 cells (5×10^4 cells per well) were incubated with the UV-irradiated samples, and infected with HIV-1 BaL. Half of each culture supernatant of PM1 cells was harvested with subsequent addition of new UV-irradiated samples every 3 days. The replication kinetics of HIV-1 BaL was monitored by the RT assay. To assess the influence of UV-irradiation, a recombinant human RANTES that had been exposed to a UV-source was also used.

2.7. In vitro challenge experiment

To assess whether the pre-inoculation with SHIV-RANTES inhibits R5-tropic HIV-1 replication, the SHIV-RANTES-infected C8166-CCR5 cells were challenged with HIV-1 BaL. C8166-CCR5 cells were pre-infected with SHIV-RANTES or SHIV-NI at 6 days before HIV-1 BaL infection. The inoculation of SHIV-RANTES and SHIV-NI were adjusted to the same RT levels. C8166-CCR5 cells were incubated for 2 h with SHIVs, washed two times with RPMI medium, and then cultured at 5×10^4 cells per well in a 96-well plate. Six days later, the SHIV-NI- and SHIV-RANTES-infected cells were co-infected with HIV-1 BaL. The culture supernatants of the C8166-CCR5 cells were harvested every 3 days. The growth kinetics of HIV-1 BaL and SHIVs was independently monitored with a differentiating real-time PCR quantification assay [2,30]. Total RNAs were prepared from the culture supernatants of virus-infected C8166-CCR5 cells with a QIAamp viral RNA kit (Qiagen,

Germany), and RT-PCR was performed using a TaqMan RT-PCR kit (Perkin–Elmer). The SIV *gag* region of the viral RNAs of SHIV-NI and SHIV-RANTES were amplified using the primers SIVII-696F (5'-GGAAATTACCCAGTACAA-CAAATAGG-3') and SIVII-784R (5'-TCTATCAATTTT-ACCCAAGGCATTTA-3'). A labeled probe SIVII-731T (5'-Fam-TGTCCACCTGCCATTAAGCCCG-Tamra-3') was used to quantify the PCR product. To detect RNA of the challenge virus HIV-1 BaL, nucleotide sequences for the HIV-1 *gag* region were amplified using the primers NL432-gag-F (5'-CAAGCAGCCATGCAAATGTTA-3') and NL432-gag-R (5'-GCATGCACTGGATGCAATCTAT-3'). A labeled probe NL432-gag-T (5'-Fam-AGAGACCATCAATGAGGAA-GCTGCAGAATG-Tamra-3') was added to the reaction mixture. These reactions were performed with a Prism 7700 Sequence Detector (Applied Biosystems, Foster City, CA) and analyzed using the manufacturer's software. The viral RNA loads were quantified based on the copy number of the standard samples.

2.8. Stability of SHIV-RANTES after serial passages in vitro

SHIV-RANTES was inoculated to M8166 cells at 5×10^5 cells per well in a 24-well plate. When the cytopathic effect (CPE) was confluent, half of each culture supernatant was used to infect a well containing fresh M8166 cells. The culture supernatants from SHIV-RANTES-infected cells were passaged 10 times in this way. To analyze the inserted RANTES genes in SHIV-RANTES, the proviral DNA was amplified from the virus-infected cells after each passage and the length of the RANTES flanking region were checked by PCR [31].

3. Results

3.1. Replication of SHIV-RANTES and production of RANTES in human and monkey cells

In this study, a chimeric simian–human immunodeficiency virus having RANTES gene (SHIV-RANTES) was constructed (Fig. 1). SHIV-RANTES replicated well in human M8166 cells with almost the same replication competence as parental SHIV-NI (Fig. 2A). The RT activity of SHIV-RANTES peaked at about 9 days post infection (d.p.i.). The maximum level of RANTES in the culture supernatants was 98.5 ng/ml for the SHIV-RANTES-infected M8166 cells. The spontaneous production of RANTES was detected at levels between 4.1 and 9.3 ng/ml in the SHIV-NI-infected M8166 cells and the virus-uninfected M8166 cells control. Replication of SHIV-RANTES in monkey HSC-F cells, reached a peak at about 15 d.p.i. (Fig. 2B). The replication kinetics of SHIV-RANTES was similar to that of SHIV-NI. The maximum level of RANTES in the culture supernatants from SHIV-RANTES-infected HSC-F cells was at 4.1 ng/ml,

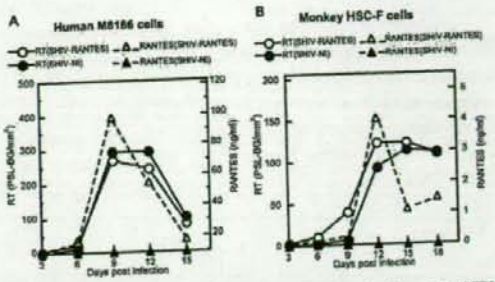

Fig. 2. Kinetics of virus replication and RANTES production with SHIV-RANTES and SHIV-NI in human (A) and monkey (B) $CD4^+$ cell lines. Viral replication was monitored by RT activity in the supernatant of cell cultures infected with SHIV-RANTES (open circles) or SHIV-NI (closed circles). The unit for RT activity is PSL-BG, photo-stimulated luminescence minus background (FLA-3000, Fuji Film, Japan). RANTES production (ng/ml) was detected by ELISA in the supernatant of cell cultures infected with SHIV-RANTES (open triangles) or SHIV-NI (closed triangles).

while it was less than the cut-off value (0.094 ng/ml) in the culture supernatants from the SHIV-NI-infected cells. SHIV-NI and SHIV-RANTES used CD4 and CXCR4, but not CCR5, as determined by an infection of GHOST cells expressing CXCR4 or CCR5 (data not shown). These data show that RANTES was produced efficiently along with the replication of SHIV-RANTES in human and monkey cells, and that the replications of SHIV-RANTES, X4-tropic virus, was not influenced by its production of RANTES.

3.2. Down-modulation of CCR5 by RANTES

RANTES down-modulates CCR5 from the cell surface, and CCR5 reaccumulates on the cell surface after the removal of ligands [29,32]. To check the biological activity of the produced RANTES, the down-modulation of CCR5 on PM1 cells was monitored. Surface expression of CCR5 was detectable on approximately 21% of PM1 cells with the anti-CCR5 MAb 2D7, which is consistent with a previous report [33]. In this study, the levels of RANTES in the cultures infected by SHIV-RANTES, SHIV-NI, and Mock were 14, 2.6, and 2.6 ng/ml, respectively. Treating the cells with recombinant human RANTES reduced expression of CCR5 on the cell surface in a dose-dependent manner (Fig. 3). When the PM1 cells were incubated with the culture supernatants from the SHIV-RANTES-infected cells, CCR5 expression on the cell surface was consistently reduced about 75%. Down-modulation of CCR5 was also observed in the cells treated with the culture supernatants from the SHIV-NI-infected cells, but the reduction was only about 33%, which was less than that in cells treated with culture supernatants from the SHIV-RANTES-infected cells. The down-modulation of CCR5 with the sample from the SHIV-NI-infected cells is thought to be due to the background concentration of RANTES, since the reduction was almost the same as that treated with the samples from the Mock (the down-modulation of CCR5 was 34%). Pretreatment of the samples with the anti-RANTES antibody

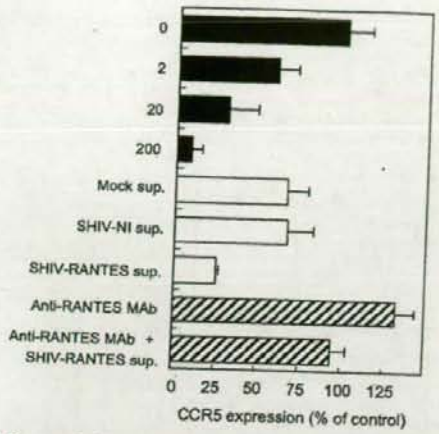

Fig. 3. Down-modulation of CCR5 on the surface of PM1 cells by RANTES. White bars, CCR5 expression on PM1 cells exposed to supernatant from cells infected with SHIV-RANTES, SHIV-NI, and uninfected cells (Mock). Black bars, PM1 cells treated with recombinant human RANTES at the indicated concentrations (in ng/ml). Hatched bars, cells treated with anti-RANTES antibody (Anti-RANTES MAb). These data are expressed as the mean of triplicate experiments ± S.E.M.

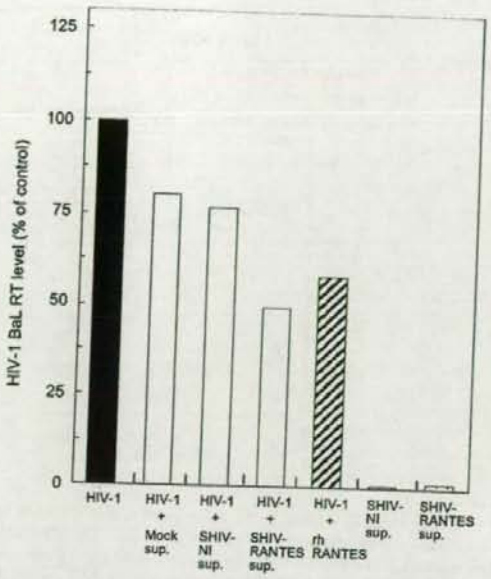

Fig. 4. Inhibition of HIV-1 BaL by UV-irradiated culture supernatants from SHIV-RANTES-infected cells. Virus replication of HIV-1 BaL was monitored by RT activity from the culture supernatants of virus-infected PM1 cells at 12 d.p.i. As control, cells treated with the same concentrations of UV-irradiated recombinant human RANTES were monitored (HIV-1 + rh RANTES). UV-irradiated supernatants from SHIV-RANTES and SHIV-NI-infected cells without HIV-1 BaL infection were used as negative controls. These data show one of three independent experiments with similar results.

completely abolished the down-modulation of CCR5. Thus, the reduction of the cell surface CCR5 correlates with the level of the expressed RANTES from SHIV-RANTES-inoculated cells.

3.3. Inhibition of R5-tropic HIV-1 BaL infection by RANTES from SHIV-RANTES-inoculated cells

In this study, the levels of RANTES in the UV-irradiated samples from the cultures infected with SHIV-RANTES, SHIV-NI, and Mock were 14, 0.8, and 0.8 ng/ml, respectively. In the case of the culture supernatants from SHIV-RANTES-infected cells, approximately 51% of the inhibition of HIV-1 BaL infection was consistently observed at 12 d.p.i., when the viral loads of the HIV-1 BaL peaked (Fig. 4). A reduction of the HIV-1 BaL RT activity was also observed for the culture supernatants from the SHIV-NI-inoculated cells and that of the Mock-inoculated cells, but the reductions were only about 23% and 20%, respectively. Interestingly, inhibition of HIV-1 BaL infection with the 14 ng/ml of the produced RANTES from the SHIV-RANTES-infected cells (51% inhibition) was slightly greater than inhibition with an equal concentration of recombinant human RANTES (42% inhibition). These results suggest that the produced RANTES efficiently inhibits R5-tropic HIV-1 infection.

3.4. In vitro challenge experiments of the SHIV-RANTES inoculated cells with R5-tropic HIV-1

A previous finding in the SIV-macaque models suggested that the induction of a CC-chemokine by a recombinant SIV vaccine was associated with protective immunity to mucosal infection with SIV [34]. We assessed whether the pre-inoculated cells with SHIV-RANTES were protected against the challenge with R5-tropic HIV-1 in in vitro experiments. In this assay, C8166-CCR5 cells were used as CCR5 positive cells, since the ability of virus replication in C8166-CCR5 cells was better than that in PM1 cells. As shown in Fig. 5A,B, the SHIV-RANTES-inoculated C8166-CCR5 cells produced RANTES, reaching a maximum level of 66.7 ng/ml at 6 days post challenge (d.p.c.) (at 12 d.p.i.). At the time of the challenge with HIV-1 BaL, the RANTES level in the culture supernatant of SHIV-RANTES-infected cells was already 16.9 ng/ml, while that of the SHIV-NI-infected cells was less than the cut-off value (2.5 ng/ml) during the experiment.

As shown in Fig. 5B, the viral loads of HIV-1 in the naive HIV-1 BaL-infected C8166-CCR5 cells increased to above 10^7 copies per ml at 9 d.p.c., and remained at a high level. Pre-inoculation of SHIV-RANTES suppressed the challenge of HIV-1 BaL. The peak virus loads of HIV-1 BaL in the SHIV-RANTES pre-inoculated C8166-CCR5 cells were two orders of magnitude lower than that of the naive HIV-1 BaL-inoculated cells. The viral loads of HIV-1 BaL in the culture supernatants of the SHIV-RANTES pre-inoculated cells plateaued at 10^4 copies per ml during the observation period. Viral loads of HIV-1 BaL in the SHIV-NI pre-infected cells reached between 10^5 and 10^6 copies per ml, which is higher

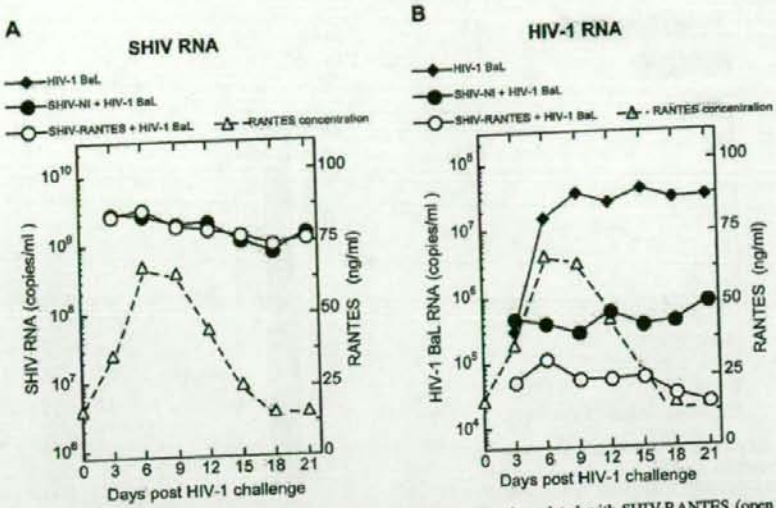

Fig. 5. Suppression of HIV-1 BaL by the pre-inoculation of SHIV-RANTES. Cells were pre-inoculated with SHIV-RANTES (open circles) and SHIV-NI (closed circles) at 6 days before the challenge of HIV-1 BaL. The HIV-1 BaL-infected cells without a pre-inoculation of SHIVs were used as a naive control (closed diamonds). Viral RNA levels of HIV-1 BaL and SHIVs were independently monitored by real-time RT-PCR using specific primer sets for either SIV *gag* region (A) or HIV *gag* region (B). Open triangles indicate RANTES levels produced by SHIV-RANTES, as determined by ELISA. (The RNA level of HIV-1 BaL detected by the primer for the SIV *gag* region was below 10^6 copies per ml).

than that in the SHIV-RANTES pre-inoculated cells. These results show that pre-inoculation of C8166-CCR5 with SHIV-RANTES partially protected against the challenge with HIV-1 BaL in vitro.

3.5. Stability of inserted RANTES gene in SHIV

Insertion of an additional gene may be a burden for the virus itself. In other studies, some cytokine genes such as IFN-γ, IL-2, and IL-12 inserted into either SHIV or SIV were found to be deleted during long-term experiments [19,35,36]. The stability of the inserted RANTES fragments in SHIV-RANTES after serial passage was examined by PCR of proviral DNA. These experiments were done more than three times. As shown in Fig. 6A, the inserted RANTES gene was found to be stable for at least 10 passages. The peaks of RANTES production in the culture supernatants from passage 1, 5, and 10 in the SHIV-RANTES-infected cells were 78.9, 76.8, and 82.2 ng/ml, respectively (Fig. 6B). These results show that SHIV-RANTES retained the ability to produce RANTES after serial passages. Furthermore, the expressed RANTES retained its ability to down-modulate CCR5 and to protect against HIV-1 BaL infection after 10 passages (Fig. 6C,D). These results show that the inserted RANTES gene in SHIV-RANTES was functional and stable until at least the 10th passage.

4. Discussion

In this paper, we compare the in vitro properties of SHIV-RANTES with those of its parental SHIV-NI. SIV/SHIV vectors containing a cytokine gene appear to be appropriate tools for observing the effect of local production of a cytokine on virus replication, pathogenesis, and immunogenicity, especially because the inserted cytokine gene is expressed in the region where the SIV/SHIV vector replicates. Because SIV dominantly utilized CCR5 for the virus entry and RANTES would suppress its replicate, we used the SHIV-NM3rN having the Env of X4-tropic HIV-1 NL432 as a vector that expresses RANTES genes. As expected, the replication of SHIV-RANTES, X4-tropic SHIV, was not suppressed by the expressed RANTES in this experiment.

SHIV-RANTES replicated well not only in the human $CD4^+$ T cell line M8166 but also in the monkey $CD4^+$ T cell line HSC-F. In addition, SHIV-RANTES successfully replicated in monkey PBMCs (data not shown). The expression level of RANTES in human M8166 cells was very high (up to 98.5 ng/ml). The high level of expression of RANTES may be partly due to the introduction of an effective ribosomal binding sequence at the flanking region of the RANTES ORF [21] and partly due to inserting the gene at the *nef* region [37]. We previously constructed the SHIV-*vpr* vector, named SHIV-3sj, from the same parental SHIV-NM3rN. Insertion of the RANTES gene into SHIV-3sj resulted in the expression of RANTES at a maximum level of 47.4 ng/ml in the culture supernatants of virus-infected M8166 cells [20]. The expression of RANTES with the SHIV-*nef* vector was about two times higher than that with the SHIV-*vpr* vector. A high level of expression of RANTES is advantageous to study the adjuvant effect of RANTES in vivo.

The results of many studies indicate that RANTES and its analogues suppress the infection of R5-tropic lentiviruses in

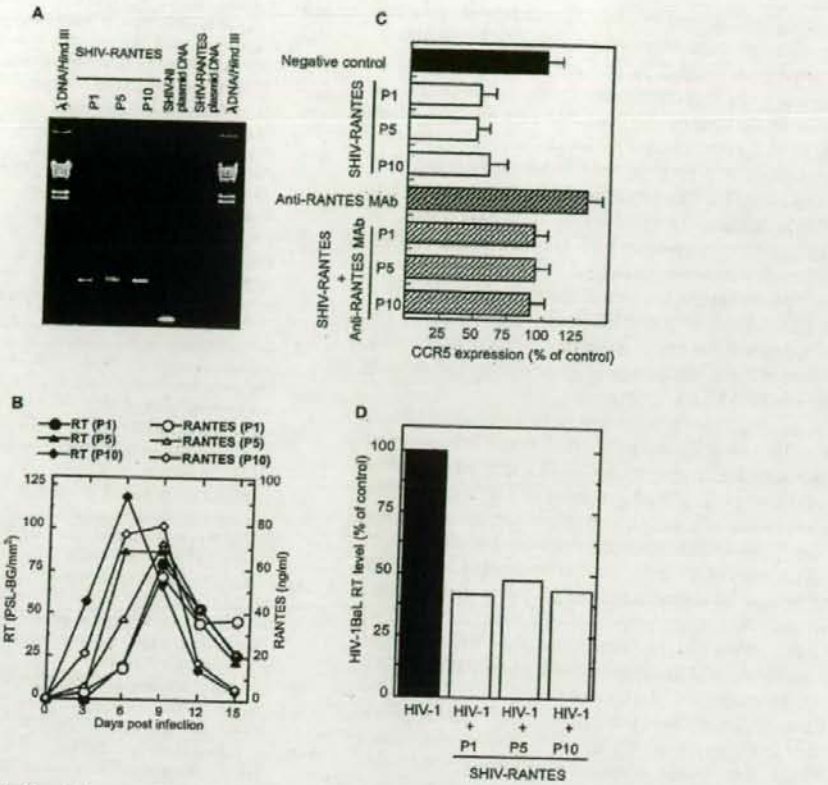

Fig. 6. Stability of SHIV-RANTES with serial passage. Culture supernatants from cells infected with SHIV-RANTES at passage 1 (P1), 5 (P5), and 10 (P10) were used for the experiments. (A) Stability of the inserted RANTES fragment in SHIV-RANTES was examined by PCR. DNA plasmids of SHIV-NI and SHIV-RANTES were used as the templates of the control. A λ DNA digested with *Hind* III was used as a size marker. (B) Kinetics of the RT activity and expression of RANTES at different passages. The unit for RT activity is PSL-BG, photo-stimulated luminescence minus background (FLA-3000, Fuji Film, Japan). The unit for RANTES (ng/ml) was determined by ELISA. (C) Down-modulation of CCR5 by RANTES expressed at different passages. The samples were also treated with anti-RANTES antibody to confirm the specificity of RANTES. (D) Inhibitory effect of R5-tripoc HIV-1 BaL replication by RANTES produced by a serial passage of SHIV-RANTES.

vitro. However, little information is available on the role of RANTES on X4-tropic lentivirus replication. Previous studies reported that RANTES enhanced X4-tropic and R5X4-tropic HIV-1 replication, both of which depend on a signal transduction and the enhanced HIV-1 replication is associated with increased colocalization of CD4 and CXCR4 [38]. The over-expression of RANTES may increase the replication of X4-tropic SHIV. A safety concern about live-attenuated viruses is that their replication rate may increase. In vitro, however, we did not observe increased SHIV replication in either human or monkey cell lines infected with the RANTES-producing virus.

Although the goal of this study is to test the immune-modulating effect of RANTES against HIV-1-related virus infection, immune responses are difficult to assess in in vitro experiments. In vitro, the inhibitory effects of RANTES on the entry of R5-tropic strains of lentivirus are well established. RANTES blocks or down-modulates CCR5 in vitro, which suppresses HIV-1 infections [29,32]. The down-modulation of CCR5 is a biological activity of RANTES. Our findings that the produced RANTES down-modulated CCR5 expression on the cell surface of PM1 cells and that UV-treated samples from SHIV-RANTES-infected cells partially protected the PM1 cells from the R5-tropic HIV-1 BaL infection suggest that RANTES expressed by SHIV-RANTES-infected cells is the factor protecting against R5-tropic HIV-1 infection. In this study, the biological activity of RANTES was confirmed by its ability to down-modulate expression of CCR5 and to inhibit the R5-tropic HIV-1 BaL infection.

Our finding that the viral growth kinetics of HIV-1 BaL was more strongly inhibited by the RANTES produced by SHIV-RANTES-infected cells than by the recombinant RANTES may be due to the presence of inactivated virus particles and other inhibitory factors in the culture supernatants of the SHIV-RANTES-inoculated cells. Another reason

is that the RANTES produced by mammalian cells is structurally different from the recombinant RANTES. RANTES is secreted from some cells as a macromolecular complex containing sulfated proteoglycans (with molecular sizes of 400–600 kDa), whereas the molecular size of recombinant RANTES is approximately 7.8 kDa [39,40]. The interaction of chemokines with proteoglycans enhances their anti-HIV-1 activity [40,41]. In this experiment, after the separation into < 100 kDa fractions by ultrafiltration (UF) membranes, the concentration of the produced RANTES was reduced to 1.6% of the pre-filtered levels (from 39.3 to 0.61 ng/ml) (data not shown). Many studies have used recombinant RANTES to determine the role of RANTES in HIV-1 infection. In our SHIV-*nef* vector system, the RANTES is produced in a natural, secreted form, which may be an advantage for studying the effect of RANTES in vivo.

The immune responses induced by an attenuated virus can increase the immunity to a pathogenic virus. Compared with the immunostimulatory cytokines produced by other *nef* deletion mutants, the RANTES produced by SHIV-RANTES is expected to not only boost the primitive non-specific immunity and virus-specific immune response but also directly inhibit the entry of R5-tropic virus to susceptible cells. SHIV-RANTES has an ability to protect against challenge with a pathogenic virus when inoculated to monkeys. Indeed, we found that HIV-1 BaL replication was two orders of magnitude lower in the cells pre-inoculated with SHIV-RANTES than in the naive HIV-1 BaL-inoculated cells.

In conclusion, we have established a SHIV-*nef* vector system that stably expresses a high level of biologically active RANTES. Inoculation of macaque monkeys with SHIV-RANTES should provide further information on the immune-modulating effects of RANTES against lentiviral infections.

Acknowledgements

We thank Dr. H. Kato, Dr. K. Maeda, and Dr. H. Nagatomo for their valuable comments and suggestions, Ms. T. Tukiyama for expert assistance with the quantitative RT-PCR, Dr. A. Krensky for providing full length RANTES cDNA, and Dr. H. Akari for providing HSC-F cells. This work was supported in part by a Grant-in-Aid for Scientific Research from the Ministry of Education and Science, Japan, a Health Sciences Research Grant from the Ministry of Health, Labor and Welfare, Japan, and a Research Grant on Health Sciences focusing on Drug innovation from the Japan Health Science Foundation.

References

[1] T. Kuwata, T. Igarashi, E. Ido, M. Jin, A. Mizuno, J. Chen, M. Hayami, Construction of human immunodeficiency virus 1/simian immunodeficiency virus strain mac chimeric viruses having vpr and/or nef of different parental origins and their in vitro and in vivo replication, J. Gen. Virol. 76 (Pt. 9) (1995) 2181–2191.

[2] Y. Enose, M. Ui, A. Miyake, H. Suzuki, H. Uesaka, T. Kuwata, J. Kunisawa, H. Kiyono, H. Takahashi, T. Miura, M. Hayami, Protection by intranasal immunization of a nef-deleted, nonpathogenic SHIV against intravaginal challenge with a heterologous pathogenic SHIV, Virology 298 (2002) 306–316.

[3] M. Ui, T. Kuwata, T. Igarashi, K. Ibuki, Y. Miyazaki, I.L. Kozyrev, Y. Enose, T. Shimada, H. Uesaka, H. Yamamoto, T. Miura, M. Hayami, Protection of macaques against a SHIV with a homologous HIV-1 Env and a pathogenic SHIV-89.6P with a heterologous Env by vaccination with multiple gene-deleted SHIVs, Virology 265 (1999) 252–263.

[4] T.W. Baba, V. Liska, A.H. Khimani, N.B. Ray, P.J. Dailey, D. Penninck, R. Bronson, M.F. Greene, H.M. McClure, L.N. Martin, R.M. Ruprecht, Live attenuated, multiply deleted simian immunodeficiency virus causes AIDS in infant and adult macaques, Nat. Med. 5 (1999) 194–203.

[5] B.R. Gundlach, M.G. Lewis, S. Sopper, T. Schnell, J. Sodroski, C. Stahl-Hennig, K. Uberla, Evidence for recombination of live, attenuated immunodeficiency virus vaccine with challenge virus to a more virulent strain, J. Virol. 74 (2000) 3537–3542.

[6] R.P. Johnson, R.C. Desrosiers, Protective immunity induced by live attenuated simian immunodeficiency virus, Curr. Opin. Immunol. 10 (1998) 436–443.

[7] L. Giavedoni, S. Ahmad, L. Jones, T. Yilma, Expression of gamma interferon by simian immunodeficiency virus increases attenuation and reduces postchallenge virus load in vaccinated rhesus macaques, J. Virol. 71 (1997) 866–872.

[8] C. Stahl-Hennig, B.R. Gundlach, U. Dittmer, P. ten Haaft, J. Heeney, W. Zou, D. Emilie, S. Sopper, K. Uberla, Replication, immunogenicity, and protective properties of live-attenuated simian immunodeficiency viruses expressing interleukin-4 or interferon-gamma, Virology 305 (2003) 473–485.

[9] F. Sallusto, A. Lanzavecchia, C.R. Mackay, Chemokines and chemokine receptors in T-cell priming and Th1/Th2-mediated responses, Immunol. Today 19 (1998) 568–574.

[10] A. Frauenschuh, A.L. DeVico, S.P. Lim, R.C. Gallo, A. Garzino-Demo, Differential polarization of immune responses by co-administration of antigens with chemokines, Vaccine 23 (2004) 546–554.

[11] J.J. Kim, L.K. Nottingham, J.I. Sin, A. Tsai, L. Morrison, J. Oh, K. Dang, Y. Hu, K. Kazahaya, M. Bennett, T. Dentchev, D.M. Wilson, A.A. Chalian, J.D. Boyer, M.G. Agadjanyan, D.B. Weiner, CD8 positive T cells influence antigen-specific immune responses through the expression of chemokines, J. Clin. Invest. 102 (1998) 1112–1124.

[12] P.M. Waterman, M. Kitabwalla, G.S. Hatfield, P.S. Evans, Y. Lu, I. Tikhonov, J.L. Bryant, C.D. Pauza, Effects of virus burden and chemokine expression on immunity to SHIV in nonhuman primates, Viral Immunol. 17 (2004) 545–557.

[13] K.Q. Xin, Y. Lu, K. Hamajima, J. Fukushima, J. Yang, K. Inamura, K. Okuda, Immunization of RANTES expression plasmid with a DNA vaccine enhances HIV-1-specific immunity, Clin. Immunol. 92 (1999) 90–96.

[14] R.K. Ahmed, C. Nilsson, Y. Wang, T. Lehner, G. Biberfeld, R. Thorstensson, Beta-chemokine production in macaques vaccinated with live attenuated virus correlates with protection against simian immunodeficiency virus (SIVsm) challenge, J. Gen. Virol. 80 (Pt. 7) (1999) 1569–1574.

[15] M.C. Gauduin, R.L. Glickman, S. Ahmad, T. Yilma, R.P. Johnson, Immunization with live attenuated simian immunodeficiency virus induces strong type 1T helper responses and beta-chemokine production, Proc. Natl. Acad. Sci. USA 96 (1999) 14031–14036 (B).

[16] J.L. Heeney, V.J. Tecuwsen, M. van Gils, W.M. Bogers, C. De Giuli Morghen, A. Radaelli, S. Barnett, B. Morein, L. Akerblom, Y. Wang, T. Lehner, D. Davis, Beta-chemokines and neutralizing antibody titers correlate with sterilizing immunity generated in HIV-1 vaccinated macaques, Proc. Natl. Acad. Sci. USA 95 (1998) 10803–10808.

[17] F. Cocchi, A.L. DeVico, A. Garzino-Demo, S.K. Arya, R.C. Gallo, P. Lusso, Identification of RANTES, MIP-1 alpha, and MIP-1 beta as the major HIV-suppressive factors produced by CD8+ T cells, Science 270 (1995) 1811–1815.

[18] G. Alkhatib, C. Combadiere, C.C. Broder, Y. Feng, P.E. Kennedy, P.M. Murphy, E.A. Berger, CC CKR5: a RANTES, MIP-1alpha, MIP-1beta receptor as a fusion cofactor for macrophage-tropic HIV-1, Science 272 (1996) 1955–1958.

[19] T. Kuwata, T. Miura, T. Haga, I. Kozyrev, M. Hayami, Construction of chimeric simian and human immunodeficiency viruses that produce interleukin 12, AIDS Res. Hum. Retroviruses 16 (2000) 465–470.

[20] T. Haga, M. Okoba, N. Yamazaki, S. Kumabe, Y. Shimizu, Y. Goto, T. Kuwata, I.L. Kozyrev, M. Hayami, T. Miura, Characterization of vpr vector constructed from chimeric simian and human immunodeficiency virus, J. Vet. Med. Sci. 65 (2003) 633–636.

[21] M. Kozak, Comparison of initiation of protein synthesis in procaryotes, eucaryotes, and organelles, Microbiol. Rev. 47 (1983) 1–45.

[22] T. Haga, Y. Shimizu, M. Okoba, S. Kumabe, Y. Goto, T. Shinjo, H. Ichimura, T. Kuwata, M. Hayami, T. Miura, Construction and in vitro properties of chimeric simian and human immunodeficiency virus with the human TNF-alpha gene, Microbiol. Immunol. 46 (2002) 849–855.

[23] P.R. Clapham, R.A. Weiss, A.G. Dalgleish, M. Exley, D. Whitby, N. Hogg, Human immunodeficiency virus infection of monocytic and T-lymphocytic cells: receptor modulation and differentiation induced by phorbol ester, Virology 158 (1987) 44–51.

[24] H. Akari, K. Mori, K. Terao, I. Otani, M. Fukasawa, R. Mukai, Y. Yoshikawa, In vitro immortalization of Old World monkey T lymphocytes with Herpesvirus saimiri: its susceptibility to infection with simian immunodeficiency viruses, Virology 218 (1996) 382–388.

[25] P. Lusso, F. Cocchi, C. Balotta, P.D. Markham, A. Louie, P. Farci, R. Pal, R.C. Gallo, M.S. Reitz Jr., Growth of macrophage-tropic and primary human immunodeficiency virus type 1 (HIV-1) isolates in a unique CD4+ T-cell clone (PM1): failure to downregulate CD4 and to interfere with cell-line-tropic HIV-1, J. Virol. 69 (1995) 3712–3720.

[26] Y. Soda, N. Shimizu, A. Jinno, H.Y. Liu, K. Kanbe, T. Kitamura, H. Hoshino, Establishment of a new system for determination of coreceptor usages of HIV based on the human glioma NP-2 cell line, Biochem. Biophys. Res. Commun. 258 (1999) 313–321.

[27] L.J. Reed, H. Muench, A simple method of estimating fifty per cent endpoints, Am. J. Hyg. 27 (1938) 493–497.

[28] S. Gartner, P. Markovits, D.M. Markovitz, M.H. Kaplan, R.C. Gallo, M. Popovic, The role of mononuclear phagocytes in HTLV-III/LAV infection, Science 233 (1986) 215–219.

[29] M. Mack, B. Luckow, P.J. Nelson, J. Cihak, G. Simmons, P.R. Clapham, N. Signoret, M. Marsh, M. Stangassinger, F. Borlat, T.N. Wells, D. Schlondorff, A.E. Proudfoot, Aminooxypentane-RANTES induces CCR5 internalization but inhibits recycling: a novel inhibitory mechanism of HIV infectivity, J. Exp. Med. 187 (1998) 1215–1224.

[30] K. Suryanarayana, T.A. Wiltrout, G.M. Vasquez, V.M. Hirsch, J.D. Lifson, Plasma SIV RNA viral load determination by real-time quantification of product generation in reverse transcriptase-polymerase chain reaction, AIDS Res. Hum. Retroviruses 14 (1998) 183–189.

[31] T. Haga, T. Kuwata, I. Kozyrev, T.B. Kwofie, M. Hayami, T. Miura, Construction of an SIV/HIV type 1 chimeric virus with the human interleukin 6 gene and its production of interleukin 6 in monkey and human cells, AIDS Res. Hum. Retroviruses 16 (2000) 577–582.

[32] N. Signoret, A. Pelchen-Matthews, M. Mack, A.E. Proudfoot, M. Marsh, Endocytosis and recycling of the HIV coreceptor CCR5, J. Cell Biol. 151 (2000) 1281–1294.

[33] L. Wu, G. LaRosa, N. Kassam, C.J. Gordon, H. Heath, N. Ruffing, H. Chen, J. Humblias, M. Samson, M. Parmentier, J.P. Moore, C.R. Mackay, Interaction of chemokine receptor CCR5 with its ligands: multiple domains for HIV-1 gp120 binding and a single domain for chemokine binding, J. Exp. Med. 186 (1997) 1373–1381.

[34] T. Lehner, Y. Wang, M. Cranage, L.A. Bergmeier, E. Mitchell, L. Tao, G. Hall, M. Dennis, N. Cook, R. Brookes, L. Klavinskis, I. Jones, C. Doyle, R. Ward, Protective mucosal immunity elicited by targeted iliac lymph node immunization with a subunit SIV envelope and core vaccine in macaques, Nat. Med. 2 (1996) 767–775.

[35] L.D. Giavedoni, T. Yilma, Construction and characterization of replication-competent simian immunodeficiency virus vectors that express gamma interferon, J. Virol. 70 (1996) 2247–2251.

[36] B.R. Gundlach, H. Linhart, U. Dittmer, S. Sopper, S. Reiprich, D. Fuchs, B. Fleckenstein, G. Hunsmann, C. Stahl-Hennig, K. Uberla, Construction, replication, and immunogenic properties of a simian immunodeficiency virus expressing interleukin-2, J. Virol. 71 (1997) 2225–2232.

[37] M. Robert-Guroff, M. Popovic, S. Gartner, P. Markham, R.C. Gallo, M.S. Reitz, Structure and expression of tat-, rev-, and nef-specific transcripts of human immunodeficiency virus type 1 in infected lymphocytes and macrophages, J. Virol. 64 (1990) 3391–3398.

[38] A. Kinter, A. Catanzaro, J. Monaco, M. Ruiz, J. Justement, S. Moir, J. Arthos, A. Oliva, L. Ehler, S. Mizell, R. Jackson, M. Ostrowski, J. Hoxie, R. Offord, A.S. Fauci, CC-chemokines enhance the replication of T-tropic strains of HIV-1 in CD4(+) T cells: role of signal transduction, Proc. Natl. Acad. Sci. USA 95 (1998) 11880–11885.

[39] T.J. Schall, J. Jongstra, B.J. Dyer, J. Jorgensen, C. Clayberger, M.M. Davis, A.M. Krensky, A human T cell-specific molecule is a member of a new gene family, J. Immunol. 141 (1988) 1018–1025.

[40] L. Wagner, O.O. Yang, E.A. Garcia-Zepeda, Y. Ge, S.A. Kalams, B.D. Walker, M.S. Pasternack, A.D. Luster, Beta-chemokines are released from HIV-1-specific cytolytic T-cell granules complexed to proteoglycans, Nature 391 (1998) 908–911.

[41] T. Oravecz, M. Pall, J. Wang, G. Roderiquez, M. Ditto, M.A. Norcross, Regulation of anti-HIV-1 activity of RANTES by heparan sulfate proteoglycans, J. Immunol. 159 (1997) 4587–4592.

Ruuska T, Vesikari T. 1990. Rotavirus disease in Finnish children: Use of numerical scores for clinical severity of diarrhoeal episodes. Scand J Infect Dis 22:259–267.

Santos N, Hoshino Y. 2005. Global distribution of rotavirus serotypes/genotypes and its implication for the development and implementation of an effective rotavirus vaccine. Rev Med Virol 15:29–56.

Santos N, Gouvea V, Timenetsky MC, Clark HF, Riepenhoff-Talty M, Garbarg-Chenon A. 1994. Comparative analysis of VP8* sequences from rotaviruses possessing M37-like VP4 recovered from children with and without diarrhoea. J Gen Virol 75:1775–1780.

Steyer A, Poljsak-Prijatelj M, Barlic-Maganja D, Jamnikar U, Mijovski JZ, Marin J. 2007. Molecular characterization of a new porcine rotavirus P genotype found in an asymptomatic pig in Slovenia. Virology 359:275–282.

Varghese V, Das S, Singh NB, Kojima K, Bhattacharya SK, Krishnan T, Kobayashi N, Naik TN. 2004. Arch Virol 149:155–172.

Vesikari T, Ruuska T, Koivu HP, Green KY, Flores J, Kapikian AZ. 1991. Evaluation of the M37 human rotavirus vaccine in 2- to 6-month-old infants. Pediatr Infect Dis J 10:912–917.

Glycobiology vol. 17 no. 7 pp. 784–794, 2007
doi:10.1093/glycob/cwm031
Advance Access publication on March 16, 2007

Changes in glycosylation of vitronectin modulate multimerization and collagen binding during liver regeneration

Kotone Sano[2], Kimie Asanuma-Date[2], Fumio Arisaka[3], Shunji Hattori[4], and Haruko Ogawa[1,2]

[2]Graduate school of Humanities and Sciences and The Glycoscience Institute, Ochanomizu University, 2-1-1 Otsuka, Bunkyo-ku, Tokyo, 112-8610 Japan; [3]Graduate School of Bioscience and Biotechnology, Tokyo Institute of Technology, 4259 Nagatsuta-cho, Midori-ku, Yokohama, 226-8502, Japan; and [4]Nippi Research Institute of Biomatrix, 1-1, Senju-midoricho, Adachi-ku, Tokyo 120-8601, Japan

Received on February 20, 2007; revised on February 20, 2007; accepted on March 9, 2007

Elucidating the mechanisms and factors regulating multimerization is biologically important in order to modulate the biological activities of functional proteins, especially adhesive proteins in the extracellular matrix (ECM). Vitronectin (VN) is a multifunctional glycoprotein present in plasma and ECM. Linkage of cellular adhesion and fibrinolysis by VN plays an essential role during tissue remodeling. Our previous study determined that the collagen-binding activity of VN was markedly enhanced with the decreased glycosylation during liver regeneration. This study demonstrated how alternations of glycans modulate the biological activity of VN. Human and rat VNs were used because of their similarities in structure and activities. The binding affinity of human VN to immobilized collagen was shown to be higher at pH 4.5 than at 7.5, at 37 °C than at 4 °C. Sedimentation velocity studies indicated that the greater the multimerization of human VN, the better it bound to collagen. The results indicate that the collagen binding of VN was modulated through its multimerization. Stepwise trimming of glycan with various exoglycosidases increased both the multimer size and the collagen binding of human VN, indicating that they are modulated by changes in glycosylation. The multimer sizes of VN purified from plasma of partially hepatectomized (PH) rats and sham-operated (SH) rats increased by about 45 and 31%, respectively, compared with those of nonoperated (NO) rats. In accordance with this, PH-VN exhibited remarkably enhanced collagen binding than SH-VN and NO-VN on surface plasmon resonance. In the PH rat sera, the multimer VN was increased in both amount and size compared with those in SH- and NO-sera. The results demonstrate that glycan alterations during tissue remodeling induce increased multimerization state to enhance the biological activity of VN.

Key words: vitronectin/multimerization/oligosaccharide/partial hepatectomy/collagen binding/multivalent effect

[1]To whom correspondence should be addressed; Tel: 03-5978-5343; Fax: 03-5978-5343; E-mail: ogawa.haruko@ocha.ac.jp

Introduction

The extracellular matrix (ECM) surrounding cells plays an important role in many biological and pathological processes, including inflammation, tissue remodeling, and invasion by cancer cells (DeClerck et al. 2004). The ECM is composed of many kinds of adhesive glycoproteins that regulate cellular signaling, motility, and proliferation. During tissue remodeling, the glycoconjugates synthesized by cells are different from those of normal tissues owing to the changes in the expression of many proteins that are responsible for glycan synthesis, such as glycosyl transferases, glycosidases, and transporters. The nature of the link between such glycan changes and the process of tissue remodeling is still unclear.

One of the components of ECM, vitronectin (VN), is a multifunctional glycoprotein that originates mainly in hepatocytes and circulates in the blood stream at high concentrations (0.2 mg/mL in humans) (Schvartz et al. 1999). VN binds to various biological ligands and it plays a key role in tissue remodeling by regulating cell adhesion and cellular motility through binding to various types of integrins on the cell surface, and by connecting the cell behavior to the pericellular proteolysis through binding with type-1 plasminogen activator inhibitor (PAI-1), urokinase-type plasminogen activator, and urokinase receptor (Preissner and Seiffert 1998; Schvartz et al. 1999). VN also regulates blood systems related to protease cascades, such as cell lysis by complements, blood coagulation, and fibrinolysis (Preissner 1991; Seiffert 1997) through interaction with heparin and thrombin–antithrombin III complexes (Podack et al. 1977; McKeown-Longo and Panetti 1996).

Tissue VN is an active multimeric form believed to interact with various matrix ligands including proteoglycans and collagen (Preissner and Seiffert 1998), whereas most VN in plasma is an inactive monomer form and does not bind to these ligands (Izumi et al. 1989). VN acquires binding activities through a conformational transition of the native inactive form to an active form after treatment with urea, heating, or in the presence of certain ligands, such as heparin or membrane attack complex in vivo (Gebb et al. 1986; Yatohgo et al. 1988). That the activation of VN is accompanied by transition to a multimer from the inactive monomer has been shown by ultracentrifugation and gel-filtration analyses (Zhuang, Blackburn, et al. 1996; Zhuang, Li, et al. 1996). Understanding the mechanism by which VN functions in various biological events has been difficult, however, due to its conformational lability and the overlapping of most of its ligand-binding activities with those of other matrix molecules.

Recently, mice with a genetic deletion of VN have shown altered responses to tissue injury, i.e., increased wound fibrinolysis and decreased angiogenesis, that resulted in delayed

wound healing (Jang et al. 2000). This indicates the importance of VN as a multifunctional glycoprotein in tissue remodeling after injury by binding with matrix molecules and cell surface receptors. However, the binding activity of VN to matrix ligands remains ambiguous in that the collagen-binding activity of VN has been observed to be slight under physiological conditions (Gebb et al. 1986). In our preceding studies, the binding activities of human and porcine VN to collagen and sulfatide were found to be affected by changes in the glycosylation of VNs in vitro (Yoneda et al. 1998). In particular, collagen binding was markedly enhanced by the absence of *N*-glycans covalently linked to VNs.

We separately found that activation of rat VN occurs during liver regeneration after partial hepatectomy. An increase in the collagen-binding activity synchronized with the glycan changes in vivo (Uchibori-Iwaki et al. 2000). The molecular mass of VN purified from partially hepatectomized rats (PH-VN) at 24 h had shrunk to 65 kDa compared with the 68–69 kDa of VNs from nonoperated (NO) and sham-operated (SH). The reduction of molecular mass was attributed to the decrease in carbohydrate concentration of PH-VN, which was two-thirds of SH-VN and one-third of NO-VN. This was accompanied by changes in *N*-glycosylation, sialylation, and isoelectric point (pI), which shifted to 6 from 4 of NO-VN and slightly above 4 of SH-VN rats, while the amino acid composition did not change significantly among the three VNs. Related to the glycosylation changes, PH-VN exhibited three times higher binding to type I collagen than NO-VN and about two times that of SH-VN by enzyme-linked immunosorbent assay (ELISA) (Nakashima et al. 1992). There are three, two, and four potential *N*-glycosylation sites for human, porcine, and rat VNs, respectively, and the potential sites of human and porcine VNs were shown to be fully glycosylated in normal animals (Zheng et al. 1995). Because the positions of the glycosylation sites and the presence of complex-type sialylated *N*-linked glycans are highly conserved among mammalian VNs (Kitagaki-Ogawa et al. 1990; Nakashima et al. 1992), the effects of glycosylation on the biological activity may be common among mammalian VNs.

How does glycosylation activate the multifunctional glycoprotein VN during liver regeneration? Recently, changes in glycosylation have been found to regulate various biological events through conformational effects or signaling functions. The present study attempted to elucidate how changes in glycans modulate the biological activity of VN during liver regeneration. The findings provide a novel insight into the significance of protein glycosylation in regulating the biological activities expressed through the multimerization process.

Results

In this study, investigation of the activation mechanism was performed mainly using human VN due to the similarities between human and rat VNs and because rat VN cannot be obtained in sufficient quantities to perform the various ultracentrifugal analyses throughout. This study simultaneously provided several lines of evidence to demonstrate the common properties between human and rat VNs in the relationship between collagen-binding activity and glycosylation.

Factors affecting binding of VN to collagen

Human VN bound to type I collagen in a concentration-dependent manner, and the binding affinity of VN was much higher at 37 °C than 4 °C throughout the pH range examined (Figure 1A and B). As shown in Figure 1B, the collagen binding showed a sharp maximum at pH 4.5 in the range of

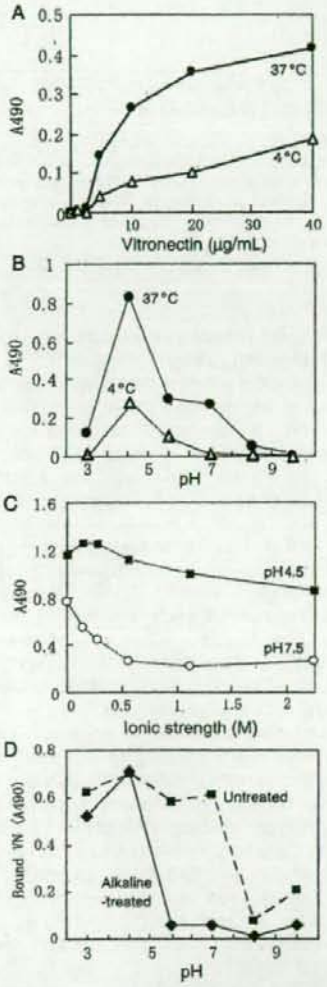

Fig. 1. Effect of concentration, temperature, pH, ionic strength, and aggregation of collagen on the collagen binding of VN. Microtiter wells were coated with type I collagen and incubated with purified human VN under various conditions. The bound VN was measured by ELISA using sheep anti-human VN IgG and HRP-conjugated rabbit anti-sheep IgG as described in the text. (**A**) Concentration dependency of VN at 37 °C (●) and 4 °C (Δ). (**B**) Effect of pH at 37 °C (●) and 4 °C (Δ). (**C**) Effect of ionic strength at pH 4.5 (■) and pH 7.5 (○). (**D**) Effect of alkaline treatment of collagen. Microtiter wells were coated with type I collagen that had been alkaline-treated to dissociate it to monomeric collagen (solid line) or untreated to remain in aggregated form (dashed line) and incubated with human VN at 37 °C. The binding activity of human VN was measured by ELISA at various pH. The data represent the average of four experiments.